Dielectric Characterization of Low-loss Materials
A Comparison of Techniques

James Baker-Jarvis, Richard G. Geyer, John H. Grosvenor, Jr.,
Michael D. Janezic, Chriss A. Jones, Bill Riddle, Claude M. Weil
Electromagnetic Fields Division, National Institute of Standards and Technology, Boulder, CO

and Jerzy Krupka
Warsaw University of Technology, Poland

ABSTRACT

Measurements on low-loss materials using closed and open cavity resonators, and dielectric resonator methods are presented. Results indicate that consistent measurement results can be obtained with a number of well-characterized fixtures. Uncertainties associated with each method are addressed. Measurements also were performed on materials used in previous intercomparisons.

1 INTRODUCTION

A goal of this paper is to present measurements on a large number of commonly used low-loss materials using a number of techniques. Good overviews describing the techniques and fixtures are found in [1–13]. We also compare and contrast measurements on the same materials using different measurement fixtures. Since each fixture operates over a frequency range, not all materials were measured at the same frequency or on all fixtures. The materials tested were ceramics, plastics, glasses, and single crystals. The intercomparison of techniques, we believe, will be very useful for reference material characterization.

When an electric field $\vec{E}$ is applied to a material, the aggregate of induced or permanent dipoles produces a net polarization in the material. The polarization is related to the displacement field by $\vec{D} = \epsilon_0 \vec{E} + \vec{P}$ where $\vec{P}$ is the polarization field density. Low-loss materials usually have little permanent dipole moment; however, they may possess appreciable induced dipole moment. Relaxation in ceramics usually results from ionic polarization, and very high permittivities can be obtained. Ionic induced polarization occurs when cations and anions in the lattice are displaced in response to the field. This displacement produces an induced dipole moment. In most polycrystalline low-loss ceramics the presence of defects which contain free radicals, produce loss. Most polymers consist of very long nonpolar molecules which have minimal dielectric response and therefore low permittivity. Loss in most plastic-like polymers results primarily from defects.

The measurement of the response of a material to an applied static or dynamic electric field allows the determination of the electric susceptibility. In weak fields, the response is linear, but in strong fields it may become nonlinear. Dielectric properties depend on frequency, homogeneity, anisotropy, temperature, and, in the case of ferroelectrics, applied dc bias field. A very readable overview to relaxation theory is the volumes by Von Hippel [4].

Field orientation is important for measurements of anisotropic materials, for example, in some single crystals. Measurement fixtures where the electric field is tangential to the air-material interfaces, such as with TE_0 cavities and dielectric resonators operated in the TE_0 mode structure, generally yield more accurate results than fixtures where the fields have a component normal to the interface. In many applications, however, it is not always possible or preferable to measure with in-plane field orientations. For example, circuit boards and printed-wiring boards operate with the electric field primarily normal to the plane of the conductors, and therefore this component of the permittivity is of paramount interest. However, measurements with the electric field normal to the sample face may suffer from air-gap depolarization. In such cases air-gap effects must be either accepted, be corrected for by numerical techniques, or mitigated by metalization. The techniques we use to mitigate air-gap effects are summarized in [3, 12]. The characterization of uniaxially anisotropic materials generally requires two techniques, two modes, or two samples, one for normal permittivity and one for in-plane permittivity components. The reentrant cavity can measure three tensor components of permittivity by use of three orthogonal axis-oriented samples. Dielectric resonators and cavity resonators measure the permittivity in the plane of the sample and therefore cannot determine any anisotropy in this plane. Dielectric rod resonators and cavities can use two different modes which have different electric field orientations to measure two orthogonal permittivity tensor components of a single sample.

Resonant methods provide high-measurement accuracy for low-loss

1070–9878/98/ $3.00

materials at microwave frequencies. Measurement inaccuracies for resonant systems are a result of air gaps between sample and metallic parts, wall losses, computational inaccuracies, and dimensional uncertainties of sample and fixture. To keep analytical solutions simple, standard geometries, such as cylindrical, spherical, or rectangular coordinates, are used where coordinate separation is possible. The solution for the permittivity usually results in a transcendental equation or determinant condition which yields the complex permittivity, given resonant frequency and quality factor.

The material under test is assumed to have a permittivity

$$\epsilon = [\epsilon_r' - j\epsilon_r'']\epsilon_o = \epsilon_r^*\epsilon_o \tag{1}$$

where ϵ_o is the permittivity of vacuum and ϵ_r^* is the complex permittivity relative to ϵ_0. In cavities and dielectric resonators the real part of the permittivity is determined from the resonant frequency through solution of a transcendental equation.

The loss tangent is determined from the quality factor measurement. The model used for loss determination includes the effects of fields both internal and external to the sample. A good review for the theory of loss determination is given by Cooke [13].

To aid in understanding the types of loss encountered in a resonant measurement, we overview here the background of loss determination. The cavity quality factor has the following form

$$\frac{1}{Q} = \frac{1}{Q_s} + \frac{1}{Q_p} \tag{2}$$

where Q_p and Q_s are the sample and parasitic quality factors. The parasitic quality factor contains all losses except those of the sample. The sample loss is contained in Q_s where

$$\frac{1}{Q_s} = p_{es} \tan \delta_s \tag{3}$$

where $\epsilon''/\epsilon' = \tan \delta_s$ is the loss tangent of the sample. The rest of the loss is in Q_p and includes radiation, wall and coupling losses

$$\frac{1}{Q_p} = p_{ed} \tan \delta_d + \frac{R_s}{G} + \frac{1}{Q_r} \tag{4}$$

Q_r is radiation loss, $\tan \delta_d$ is loss due to dielectrics other than from the sample, and R_s is the surface resistance of metal walls. The filling factor in (3 and 4) is

$$p_{ei} = \frac{W_{ei}}{W_t} = \frac{\int_V \epsilon_i |\vec{E}|^2 dV}{\int_{V_t} \epsilon |\vec{E}|^2 dV} \tag{5}$$

where $i = s, d$ indicates sample or other dielectrics in the resonator. W_{es} is the energy stored in the sample, W_{ed} is the energy stored in any dielectric support structure, and $W_t = W_{es} + W_{ed}$ is the total stored energy. The geometric factor in (4) is related to conductor loss and is defined as

$$G = \frac{\int_V \mu_0 |\vec{H}|^2 dV}{\int_S |\vec{H}_t|^2 dS} \tag{6}$$

Evaluation of conductor losses usually requires rigorous numerical computation. In addition, the surface resistance of the metal shields must be well-characterized at the frequency and temperature of the measurement.

In almost all dielectric measurement techniques it is very important to have very accurately machined samples. We have a machinist construct the samples with strict dimensional tolerances. We also measure the dimensions of the finished samples to $\pm 3 \times 10^{-6}$ m using the average of many measurements over the surface of the sample using a digital-readout dimensional probe. In cases where air gaps are important we try to mitigate the effects by metalization.

In this paper we present measurements on thin materials, but not thin films. The split-post resonator has been used for free-standing films by layering film on top of film to achieve a reasonable thickness.

2 RESONANT METHODS FOR LOW-LOSS MATERIALS

Resonant methods are the most accurate for obtaining permittivity of low-loss materials. The term 'low loss' as used in this paper refers to materials where $\tan \delta \leqslant 0.005$. Medium loss refers to materials with $0.005 \leqslant \tan \delta \leqslant 0.1$. There are limitations on the frequencies and loss characteristics of the materials that can be measured with resonant techniques. The frequencies of measurement are practically limited to the high-megahertz to gigahertz regions. Cavities operate with modes that resonate between metallic walls and therefore wall loss corrections must be made for these techniques [1]. Dielectric resonators operate with modes that resonate within the sample. Therefore dielectric resonator techniques have minimal metallic losses. Dielectric resonators allow measurements at lower frequencies than cavities since the wavelength in the material is much less than in air. The question of how thin a material can be measured by a fixture depends on the measurement technique and machining tolerances of the sample. The primary uncertainty in a thin material measurement relates to the uncertainty in the sample thickness. In most of the resonant techniques the uncertainty in permittivity is of order $\Delta L/L$. In order to obtain an accurate measurement, there must be enough material to yield an adequate frequency shift. In this paper we present results from TE_{01} 50 and 60 mm cavity resonators, whispering gallery resonators, reentrant cavity, dielectric post, split-cavity, and split-post dielectric resonators.

TE_{01} cavity resonators provide reasonably accurate measurements of low-medium-loss materials. A range of frequencies can be measured by use of a number of TE_{01n} modes or by changing cavity length. We use 50 and 60 mm mode-filtered cavities as shown in Figure 1 [1]. Samples are cylindrical in shape with the diameter the same as the cavity and typically 1 to 2 cm in height. The helical windings on the walls of the cavity allow only azimuthal current flow and thereby attenuate unwanted modes. The measurement frequencies center around 10 GHz. Tuning can be achieved over a 2 to 3 GHz range by moving the end plate. A typical quality factor for this type of cavity is 50000. Loss determination is limited by wall losses. As a result, cavity resonators are less accurate for loss measurements than dielectric resonators.

Thin materials, that is, materials $<$ 2 mm thick, can be measured nondestructively using a split TE_{011} cavity resonator (see Figure 2). The technique allows measurement at X-band frequencies for low-to-medium loss materials. This type of resonator has the electric field oriented parallel to the sample plane. The thin material is placed between the sections of the cavity and a resonant mode is excited. These resonators can be constructed of various sizes to allow operation at frequencies from 1 to 50 GHz. Typical quality factors are in the 5000 to 8000 range. Uncertainties in permittivity in split-cavity resonators are primarily influenced by sample thickness.

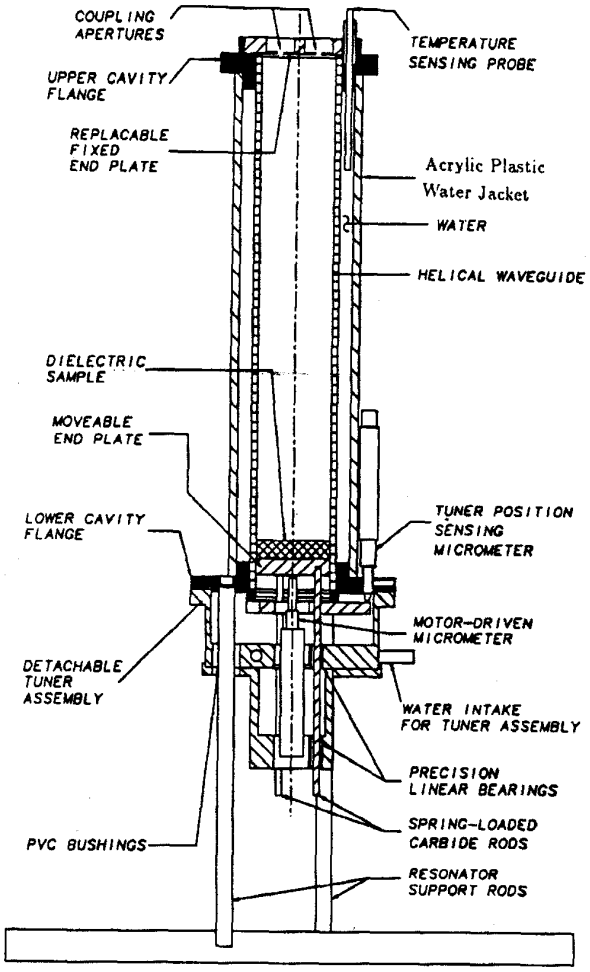

Figure 1. TE_{01} mode-filtered cavity resonator

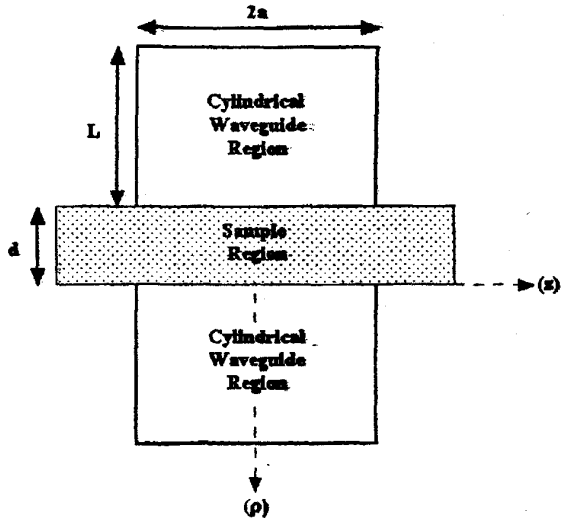

Figure 2. Split-cavity TE_{01} resonator

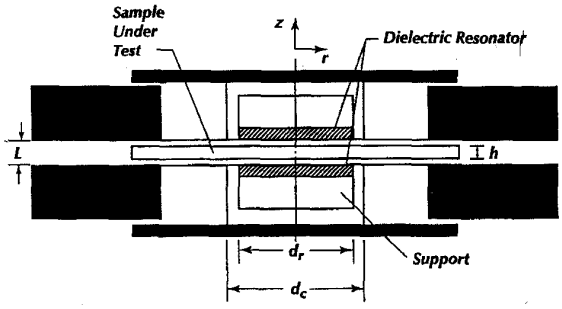

Figure 3. Split-post dielectric TE_0 resonator

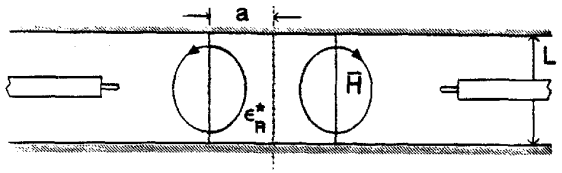

Figure 4. Parallel-plate dielectric post TE_0 resonator

The split-post TE_0 dielectric resonator as shown in Figure 3 is another technique for measurement of thin materials [14–16]. A thin material or film is inserted between the posts of the resonator. The system is then excited in the $TE_{01\delta}$ mode and a resonance of the combined post-air-material system is obtained (see Figure 3).

In this method the electric field is tangential to the plane of the sample. Numerical methods are used to analyze these measured data. A useful feature of split-post resonators is that they can be practically designed to operate at lower frequencies than TE_{01} cavities. Free-standing polymer films can be measured using the split-post resonator technique by layering the sample until the uncertainty in thickness $(\Delta L/L)$ corresponds to the requirements of the dielectric measurement.

Parallel-plate dielectric resonators as shown in Figure 4 have been used to measure low-loss dielectric and magnetic samples [17–21]. For dielectric measurements, the sample is in the form of a cylinder and resonates in the TE_{011} mode. This mode propagates in the sample, but is evanescent outside the sample. Therefore, a large amount of electrical energy can be stored in high-Q dielectric resonators. A hybrid mode also can be used to determine permittivity in the axial direction. Parallel-plate dielectric resonators can be used for magnetic measurements on thin rods surrounded by dielectric sleeves. The dielectric sleeves allow resonance at varying frequencies. Sleeves of various sizes and permittivity allow measurements from 1 to 20 GHz.

Many applications require an accurate radio-frequency measurement of the component of permittivity normal to the face of the material. Applications include measurements of circuit boards and printed-wiring boards used in computers that operate in the low megahertz region. This type of field configuration is obtainable by capacitive-type structures; however, at radio frequencies generally capacitive measurement techniques are not applicable. The reentrant cavity as indicated in Figure 5 can accurately measure materials at frequencies from 100 MHz to 2 GHz in a modified capacitor format [26–31]. An overview of the full-mode theory and measurement for the reentrant cavity is given in [31].

Table 1. Dielectric measurement techniques compared. The parasitic quality factor is Q_p, the filling factor is p_e. The parasitic quality factor contains effects from all losses except those of the sample.

Technique	f GHz	ε'_r	Air Gap	Q_p	p_e	$\tan\delta$
TE_{01} Cavity	5–50	1–500	N	10^4–10^5	0.001–0.3	10^{-5}–10^{-2}
Reentrant	0.1–2	1–50	Y	1×10^3–4×10^3	0.1–1	10^{-4}–10^{-1}
Split post	1–10	1–1000	N	0.5×10^4–4×10^4	0.01–0.3	10^{-5}–10^{-2}
Split cavity	5–50	1–500	N	2×10^4–5×10^4	0.001–0.1	10^{-5}–10^{-2}
TE_{01} Dielectric Resonator	5–50	2–10^5	N	1×10^3–2×10^4	0.9–1	10^{-5}–10^{-2}
$TE_{0\eta\delta}$ Dielectric Resonator	1–50	2–10^5	N	2×10^4–5×10^5	0.9–1	10^{-5}–10^{-3}
Whispering-Gallery Mode	5–200	10–10^5	N	10^9	0.9–1	10^{-9}–10^{-3}
Fabry-Perot	20–200	2–100	N	10^5	0.1	10^{-5}–10^{-2}

Table 2. Glass Samples. The RSS are as follows: parallel-plate dielectric resonator: $U_{\varepsilon'} = \pm0.5\%$, $U_{\tan\delta} = \pm2\times10^{-5}$, split-cavity: $U_{\varepsilon'} = \pm1\%$, $U_{\tan\delta} = \pm1\times10^{-4}$, TE_{01} cavity resonator: $U_{\varepsilon'} = \pm1\%$, $U_{\tan\delta} = \pm1\times10^{-4}$, Fabry-Perot resonator: $U_{\varepsilon'} = \pm2\%$, $U_{\tan\delta} = \pm2\times10^{-4}$, reentrant cavity: $U_{\varepsilon'} = \pm1\%$, $U_{\tan\delta} = \pm2\times10^{-4}$. Frequency f in GHz.

Material	Parameter	Parallel Plate	Split Cavity	60 mm TE_{01}	Fabry Perot	Reentrant Cavity
Corning 7980	f	5.07	8.86	9.64	60	
(batch	ε'	3.848	3.792	3.826	3.858	
34604)	$\tan\delta$	6.85×10^{-5}	4.91×10^{-4}	1.4×10^{-4}	1.70×10^{-4}	
Corning 7980	f	5.07	8.86	9.63	58.7	
(batch	ε'	3.844	3.796	3.826	3.843	
34605)	$\tan_\delta$	6.8×10^{-5}	1.48×10^{-4}	1.4×10^{-4}	5.45×10^{-4}	
Corning 7980	f	5.26	8.86	9.64	58.7	
(batch	ε'	3.844	3.799	3.826	3.832	
34606)	$\tan\delta$	6.90×10^{-5}	1.80×10^{-4}	1.3×10^{-4}	4.07×10^{-4}	
Corning 7940	f	4.89	8.86	9.64	59.9	
(batch	ε'	3.847	3.808	3.826	3.781	
44608)	$\tan\delta$	6.83×10^{-5}	1.77×10^{-4}	1.4×10^{-4}	5.09×10^{-4}	
Corning 1723	f	9				1
H. Bussey	ε'	6.20				6.21
(1959)	$\tan\delta$	5.36×10^{-3}				3.2×10^{-3}

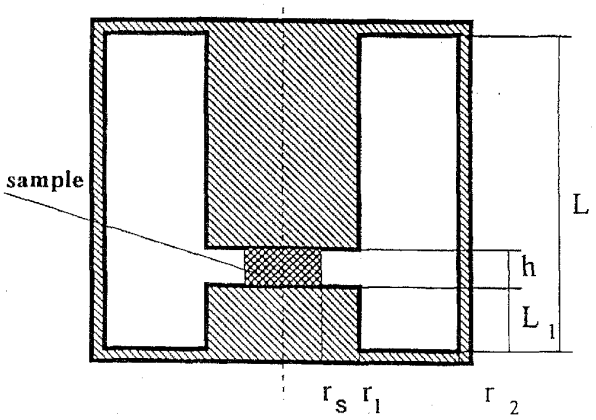

Figure 5. Re-entrant cavity

The re-entrant cavity consists of a coaxial line or other transmission line with a gap between electrodes where a sample is positioned. The cavity is then resonated and the capacitance of the gap produces a frequency shift with respect to an air measurement. Air-gap effects can be substantially reduced in these types of techniques by metalizing the faces of the sample that are in contact with the electrodes.

Low-loss dielectric materials can be measured in the microwave region by use of surface electromagnetic waves as shown in Figure 6 [9, 32–37]. In these techniques, usually the sample is supported from the bottom center with a dielectric rod, since the surface wave modes do not penetrate appreciably into the sample. Measurements using surface

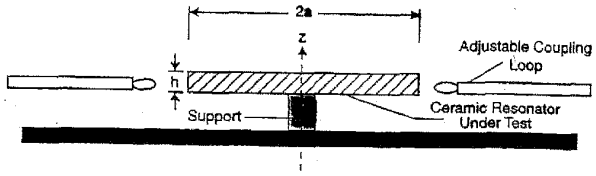

Figure 6. Whispering gallery mode resonator. The sample is in form of a disk.

waves on low-loss materials are attractive since conductor loss can be made very small. Whispering gallery modes have been used for both real permittivity and loss tangent measurements. These modes have high-order azimuthal wave numbers and propagate on concave surfaces where the waves are confined to the air-dielectric interface. These waves attenuate very rapidly with increasing depth in the material; therefore, only a thin surface layer of the sample is involved in the measurement. This is in contrast to the dielectric-post resonator where the waves penetrate the entire sample. Dielectric loss can be measured with high accuracy using the whispering gallery mode technique.

Open resonators have been used for measuring low-loss materials in the millimeter range as shown in Figure 7 [38–42]. Open resonators, such as the Fabry-Perot resonators, consist of two separated mirrors with a coupling aperture on one of the mirrors. In the confocal setup both mirrors are concave, whereas in the semi-confocal arrangement one of the mirrors is flat and the other is concave. The concave feature of the mirror minimizes radiation leakage from the open sides of the resonator and focuses the beam onto a smaller area of the sample under test,

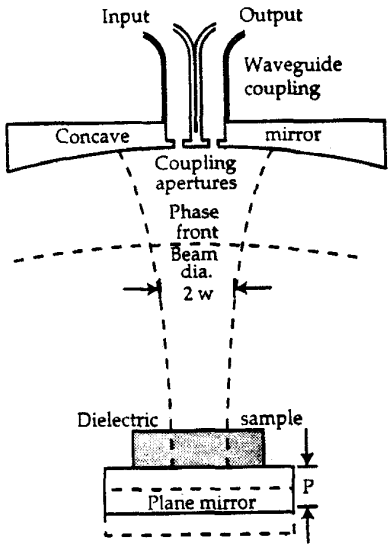

Figure 7. Fabry-Perot resonator

Table 3. Plastic Samples. The RSS are as follows: parallel-plate dielectric resonator: $U_{\varepsilon'} = \pm 0.5\%$, $U_{\tan\delta} = \pm 2\times10^{-5}$, TE_{01} cavity resonator: $U_{\varepsilon'} = \pm 1\%$, $U_{\tan\delta} = \pm 1\times10^{-4}$, reentrant cavity: $U_{\varepsilon'} = \pm 2\%$, $U_{\tan\delta} = \pm 2\times10^{-4}$

Material	Parameter	Parallel Plate	60 mm TE_{01}	Reentrant Cavity
FEP	f	6.59	9.837	
	ε'	2.064	2.025	
	$\tan\delta$	7.04×10^{-4}	3.1×10^{-4}	
PTFE	f	9.93	9.816	1.082
	ε'	2.05	2.055	2.06
	$\tan\delta$	2.0×10^{-4}	2.1×10^{-4}	$3.\times10^{-4}$
CPS	f	5.7	9.982	1.032
	ε'	2.542	2.533	2.56
	$\tan\delta$	5.1×10^{-4}	4.2×10^{-4}	7×10^{-4}
Nylon	f	4.75	9.742	
	ε'	3.08	3.01	
	$\tan\delta$	8.4×10^{-3}	7.1×10^{-3}	
PMMA	f	5.721	9.813	
	ε'	2.634	2.626	
	$\tan\delta$	7.2×10^{-3}	4.4×10^{-3}	

thereby minimizing sample edge diffraction effects. These resonators are similar to interferometers used in optical devices. Fabry-Perot resonators have large quality factors and are useful for measurements on thin, low-loss materials. The tensor permittivity values can be obtained by measuring at different angles of incidence. The metal mirrors limits the accuracy of the loss measurement.

A summary of the characteristics of the various measurement techniques used in this paper are given in Table 1.

3 MEASUREMENTS, UNCERTAINTIES, AND DISCUSSION

In Tables 2 through 6 we present measurement results on a broad spectrum of materials using various fixtures and measurement frequencies Unless referenced these measurements are new and not previously published. All measurements were performed at 22°C ± 2°C. The measurements are classified under glasses, plastics, single crystals, and ceramics. Not all materials were measured by all fixtures. The frequencies of the measurements were determined by the resonance characteristics of each fixture.

In most cases the uncertainties, denoted U_i, were calculated by the root sum-of-squares technique (RSS). In order to use the RSS method a set of independent uncertainties must be identified. These uncertainties include sample thickness and radial dimension, resonant frequency and quality factor, cavity dimensions, and coupling effects. For example, the uncertainty in the permittivity can be estimated from sample thickness h, radial dimension a, cavity length L, and resonant frequency f_r by

$$\Delta\epsilon_r' = \Big[(\tfrac{\partial\epsilon'}{\partial h}\Delta h)^2 + (\tfrac{\partial\epsilon'}{\partial L}\Delta L)^2 + (\tfrac{\partial\epsilon'}{\partial a}\Delta a)^2 + (\tfrac{\partial\epsilon'}{\partial f_r}\Delta f_r)^2 + (\tfrac{\partial\epsilon'}{\partial L_c}\Delta L_c)^2)^2\Big]^{1/2} \quad (7)$$

If the independent sources of uncertainty correspond to one standard deviation then the uncertainty in permittivity also will correspond to one standard deviation. The uncertainty in loss tangent was calculated by the RSS technique by taking partial derivatives of loss tangent with respect to independent variables. For each measurement method the appropriate partial derivatives with respect to independent variables were calculated, either numerically or analytically, and then used to form standard uncertainties. In the case of the reentrant cavity the uncertainties were calculated by comparison to measurements of previously developed reference materials.

The glasses in Table 2 were primarily fused silica with the exception of 1723 glass. The 1723 glass has been in our laboratory since the early 1960's. It has been used in two previous international comparisons [43]. We see in Table 6 that round robin tests performed in 1964 and 1972 yield similar measurement results when compared to current results. The 1964 fused-silica results in Table 6 also have not changed significantly over time.

The plastics in Table 2 include crosslinked polystyrene (CPS), polytetrafluoroethylene (PTFE), fluoroethylenepropylene (FEP), nylon, and polymethylmethacrylate (PMMA). The FEP does not have the thermal expansion phase change occurring near room temperature as does common PTFE. Some of the single-crystal materials in Table 2 are isotropic; others are uniaxially anisotropic. The anisotropic single-crystal materials were measured along two axes whenever possible.

In Table 5, the permittivity of a wide variety of low-loss ceramics is displayed. We measured two samples of alumina which have a much different loss. The loss tangent of low-loss ceramics generally increases linearly with frequency.

REFERENCES

[1] E. J. Vanzura, R. G. Geyer, and M. D. Janezic, "The NIST 60-millimeter diameter cylindrical cavity resonator: Performance evaluation for permittivity measurements", Tech. Rep., Natl. Inst. Stand. Technol. Tech. Note 1354, August 1993.

[2] I. Bahl and K. Ely, "Modern microwave substrate materials", Microwave J. (State of the Art Reference), Vol. 33, pp. 131–146, 1990.

[3] W. P. Westphal, "Techniques of measuring the permittivity and permeability of liquids and solids in the frequency range 3 c/s to 50 kMc/s", Laboratory for Insulation Research Technical Report XXXVI, MIT, 1950.

Table 4. Single Crystals. The RSS are as follows: parallel-plate dielectric resonator: $U_{\varepsilon'} = \pm 0.5\%$, $U_{\tan\delta} = \pm 2\times10^{-5}$, whispering gallery mode resonator: $U_{\varepsilon'} = \pm 0.1\%$, $U_{\tan\delta} = \pm 2\times10^{-5}$. Anisotropic materials were measured either by two dominant modes (TE_{0111} and HE_{111}) using the parallel plate rod resonator or two families of whispering gallery modes.

Material	Parallel plate			Whispering gallery		
	f, GHz	ε'	$\tan\delta$	f, GHz	ε'	$\tan\delta$
Quartz ∥c-axis	9.03	4.443	1.3×10^{-5}			
Quartz ⊥c-axis	7.75	4.59	1.3×10^{-5}			
$LaAlO_3$ (cubic)	18.38	23.99	1.0×10^{-5}			
$NdGaO_3$ (cubic)	18.49	21.82	1.07×10^{-4}			
Zirconia (cubic)	4.30	27.8	3.28×10^{-3}			
Al_2O_3 ⊥c-axis (sapphire)			2×10^{-5}	12.4	9.40	7×10^{-6}
$LiNbO_3$ ∥c-axis	10.19	32.97	$8.\times10^{-5}$			
$LiNbO_3$ ⊥c-axis	11.56	42.34	8.4×10^{-5}			
TiO_2 ∥c-axis				4.2	163.7	1×10^{-4}
TiO_2 ⊥c-axis				4.2	85.6	8×10^{-5}

Table 5. Ceramic samples: G general, A alumina. The RSS are as follows: parallel-plate dielectric resonator: $U_{\varepsilon'} = \pm 0.5\%$, $U_{\tan\delta} = \pm 2\times10^{-5}$, TE_{01} cavity resonator: $U_{\varepsilon'} = \pm 1\%$, $U_{\tan\delta} = \pm 1\times10^{-4}$, whispering gallery mode resonator: $U_{\varepsilon'} = \pm 0.1\%$, $U_{\tan\delta} = \pm 2\times10^{-5}$.

Material	Parallel plate			60 mm cavity			Whispering gallery		
	f, GHz	ε'	$\tan\delta$	f, GHz	ε'	$\tan\delta$	f, GHz	ε'	$\tan\delta$
C 4	3.675	4.704	6.8×10^{-4}	9.76	4.686	5.8×10^{-4}			
C 6	3.17	6.592	4.58×10^{-4}	9.74	6.592	5.3×10^{-4}			
C 9	2.713	9.808	2.55×10^{-4}	9.74	9.73	2.5×10^{-4}			
A 1968	3.27	10.04	3.9×10^{-5}	9.53	10.02	3.3×10^{-5}	9.528	9.98	3.2×10^{-5}
A 1996				9.00	9.992	5.3×10^{-4}			
C 13	1.987	13.51	1.07×10^{-4}	9.72	13.55	1.1×10^{-4}	9.577	13.54	1.0×10^{-4}
C 16	1.834	16.60	2.4×10^{-5}	9.71	16.64	4×10^{-5}	9.692	16.66	5.7×10^{-5}
C 20	1.617	20.77	8.4×10^{-5}	9.70	20.80	2.0×10^{-4}			
C 31	1.328	30.96	2.4×10^{-5}	9.44	31.03	5.0×10^{-5}	6.023	30.99	4.9×10^{-5}
C 35	1.200	35.15	4.8×10^{-5}	9.46	35.19	1.6×10^{-4}	5.460	35.14	1.2×10^{-4}
C 36	1.116	36.55	3.3×10^{-5}	9.46	36.56	1.2×10^{-4}	4.812	36.55	8.8×10^{-5}
C 38	1.109	38.65	5.8×10^{-5}	9.73	38.77	3.0×10^{-4}			
C 78	2.83	78.29	3.1×10^{-4}						
C 79	0.855	79.27	1.63×10^{-4}	9.44	79.29	7.8×10^{-4}	4.448	79.11	4.40×10^{-4}
C 86	0.854	86.61	3.24×10^{-4}	9.70	86.85	14.8×10^{-4}			

Table 6. Previous round robin measurements compared with recent measurements. The round-robin results from 1965 are given for NBS and NPL. The RSS are as follows: parallel-plate dielectric resonator: $U_{\varepsilon'} = \pm 0.5\%$, $U_{\tan\delta} = \pm 2\times10^{-4}$, TE_{01} cavity resonator: $U_{\varepsilon'} = \pm 1\%$, $U_{\tan\delta} = \pm 1\times10^{-4}$

Material	Paramater	$NBS(1964)$	*ParallelPlate*	$TE_{01}(50mm)$	$TE_{01}(60mm)$
$1723Glass$	f	9		10	
$H.Bussey$	ε'	6.20		6.26	
$(1964RR)$	$\tan\delta$	5.3×10^{-3}		4.8×10^{-3}	
$1723Glass$	f	9		9.58	10
$H.Bussey$	ε'	6.155		6.16	6.146
$(1972RR)$	$\tan\delta$	4.7×10^{-3}		4.9×10^{-3}	4.7×10^{-3}
$7940Glass$	f	9	9	10	9.82
$H.Bussey$	ε'	3.826	3.822	3.828	3.829
$(1972RR)$	$\tan\delta$	1.2×10^{-4}	1.4×10^{-4}	1.03×10^{-4}	1.2×10^{-4}

[4] A. R. V. Hippel, *Dielectric Materials and Applications*. Cambridge, MA: M.I.T. Press, 1954.

[5] J. Baker-Jarvis, "Transmission/reflection and short-circuit line permittivity measurements", Tech. Rep., Natl. Inst. Stand. Technol. Tech. Note 1341, July 1990.

[6] J. Baker-Jarvis, E. Vanzura, and W. Kissick, "Improved Technique for Determining Complex Permittivity with the Transmission/Reflection Method", IEEE Trans. Microwave Theory Tech., Vol. 38, pp. 1096–1103, August 1990.

[7] J. Krupka and A. Kedzior, "Optimization of the complex permittivity measurement of low loss dielectrics in a cylindrical $TE_0 1n$ mode cavity", Electron. Tech., Vol. 14, pp. 67–79, 1981. Presented at Canterbury, UK.

[8] J. Krupka and A. Kedzior, "Optimization of the complex permittivity measurement of low loss dielectrics in a cylindrical $TE01$ mode cavity", Electron. Tech., Vol. 14, pp. 67–79, 1981.

[9] J. Krupka, D. Cros, M. Aubourg, and P. Guillon, "Study of whispering gallery modes in anisotropic single-crystal dielectric resonators", IEEE Trans. Microwave Theory Tech., Vol. 42, no. 1, pp. 56–61, 1994.

[10] J. Krupka, S. Pietruszko, R. G. Geyer, J. Baker-Jarvis, and K. Derzakowski, "Measurement of the complex permittivity of microwave circuit board substrates using split dielectric resonator and reentrant cavity techniques", in Seventh International Conference on Dielectric Materials, Measurements and Applications, pp. 21–24, 1996.

[11] C. S. Chang and A. P. Agrawal, "Fine line thin dielectric circuit board characterization", in 44th Electronic Components and Technology Conference, pp. 564–569, Components, Hybrids and Manufacturing Technology Society, 1994.

[12] J. Baker-Jarvis, M. D. Janezic, J. H. Grosvenor, and R. G. Geyer, "Transmission/reflection and short-circuit line methods for measuring permittivity and permeability", Natl. Inst. Stand. Technol. Tech. Note 1355, National Institute of Standards and Technology, 1992.

[13] R. J. Cook, *Microwave cavity methods*, pp. 12–27. IPC Science and Technology Press, 1973.

[14] Y. Kobayashi and M. Katoh, "Microwave measurement of dielectric properties of low-loss materials by the dielectric rod resonator method", IEEE Trans. Microwave Theory Tech., Vol. MTT-33, pp. 586–592, 1985.

[15] T. Nishikawa, H. Tanaka, and Y. Ishikawa, "Noncontact relative measurement method for complex permittivity of ceramic substrate", IECE of Japan Symposium Digest, pp. 154–155, 1986.

[16] S. Maj and M. Pospieszalski, "A composite multilayered cylindrical dielectric resonator", in MTT-S Digest, pp. 190–192, IEEE, May 1984.

[17] B. W. Hakki and P. D. Coleman, "A dielectric resonator method of measuring inductive capacities in the millimeter range", IEEE Trans. Microwave Theory Tech., Vol. MTT-8, pp. 402–410, July 1960.

[18] W. E. Courtney, "Analysis and evaluation of a method of measuring the complex permittivity and permeability of microwave insulators", IEEE Trans. Microwave Theory Tech., Vol. MTT-18, pp. 467–485, August 1970.

[19] Y. Kobayashi, "Resonant modes of a dielectric rod resonator short-circuited at both ends by parallel conducting plates", IEEE Trans. Microwave Theory Tech., Vol. MTT-28, pp. 1077–1085, October 1980.

[20] J. Krupka, "Computations of frequencies and intrinsic Q factors of $TE01n$ modes of dielectric resonators", IEEE Trans. Microwave Theory Tech., Vol. MTT-33, pp. 274–277, March 1985.

[21] Y. Kobayashi, "Resonant modes in shielded uniaxial-anisotropic dielectric rod resonators", IEEE Trans. Microwave Theory Tech., Vol. MTT-41, pp. 2198–2204, December 1993.

[22] J. Krupka, F. Derzakowski, and J. Modelski, "Method of measuring the complex permittivity and permeability of ferrite substrate plates by means of two section dielectric resonator with TE01δ mode", in MIKON Digest, pp. 393–397, September 1991. Presented at MIKON, Poland.

[23] J. Krupka, K. Derakowski, A. Abramowicz, M. Tobar, and R. Geyer, "Whispering gallery modes for complex permittivity measurements of ultra-low loss dielectric materials", submitted to IEEE Trans. Instrum. Meas., 1998. .

[24] J. Krupka, R. G. Geyer, M. Kuhn, and J. H. Hinken, "Dielectric properties of single crystals of $A_{l2}O_3$, LaAlO, $NdGaO_3$, $SrTiO_3$, and MgO at cryogenic temperatures", IEEE Trans. Microwave Theory Tech., Vol. 42, no. 10, pp. 1886–1890, 1994.

[25] R. G. Geyer and J. Krupka, "Dielectric properties of materials at cryogenic temperatures and microwave frequencies", in CPEM'94 Digest, pp. 350–351, Conference on Precision Electromagnetic Measurements, 1994.

[26] R. D. Harrington, R. C. Powell, and P. H. Haas, "A re-entrant cavity for measurement of complex permeability in the very-high frequency region", J. Res. Nat. Bur. Stand., Vol. 56, no. 3, pp. 129–133, 1956.

[27] C. N. Works, T. W. Dakin, and F. W. Boggs, "A resonant cavity method for measuring dielectric properties at ultra-high frequencies", AIEE Trans., Vol. 63, pp. 1092–1098, 1944.

[28] W. Xi, W. R. Tinga, W. A. G. Voss, and B. Q. Tian, "New results for coaxial re-entrant cavity with partially dielectric filled gap", IEEE Trans. Microwave Theory Tech., Vol. MTT-40, pp. 747–753, April 1992.

[29] A. Kaczkowski and A. Milewski, "High-accuracy wide-range measurement method for determination of complex permittivity in re-entrant cavity: Part A- theoretical analysis of the method", IEEE Trans. Microwave Theory Tech., Vol. MTT-28, no. 3, pp. 225–228, 1980.

[30] A. Kaczkowski and A. Milewski, "High-accuracy wide-range measurement method for determination of complex permittivity in reentrant cavity: Part B- experimental analysis of measurement errors", IEEE Trans. Microwave Theory Tech., Vol. MTT-28, no. 3, pp. 228–231, 1980.

[31] J. Baker-Jarvis and B. F. Riddle, "Dielectric measurements using a reentrant cavity", Tech. Rep., Natl. Inst. Stand. Technol. Tech. Note 1384, November 1996.

[32] L. Rayleigh, "The problem of the whispering galley", Phil. Mag., Vol. 20, pp. 1001–1004, 1910.

[33] J. R. Wait, "Electromagnetic whispering-gallery modes in a dielectric rod", Radio Sci., Vol. 2, pp. 1005–1017, 1967.

[34] C. Vedrenne and J. Arnaud, "Whispering-galley modes of dielectric resonators", IEE Proc. H, Vol. 129, pp. 183–187, August 1982.

[35] J. Delaballe, "Complex permittivity measurement of mic substrates", Electronics and Telecommunications, Vol. 35, pp. 80–83, 1981.

[36] O. Weiming, C. G. Gardner, and S. A. Long, "Nondestructive measurement of a dielectric layer using surface electromagnetic waves", IEEE Trans. Microwave Theory Tech., Vol. MTT-31, pp. 255–260, March 1983.

[37] J. R. W. Alexander and R. J. Bell, "The use of surface electromagnetic waves to measure material properties", J. Noncryst. Solids, Vol. 19, pp. 93–103, 1975.

[38] A. C. Lynch, "Precise measurement of complex permittivity and permeability in the millimeter region by a frequency domain technique", IEEE Trans. Instrum. Meas., Vol. 23, pp. 425–430, 1974.

[39] M. A. Afsar, "Dielectric measurements of millimeter-wave materials", IEEE Trans. Microwave Theory Tech., Vol. MTT-32, pp. 1598–1609, 1984.

[40] H. Kogelnik and T. Li, "Laser beams and resonators", Proceedings IEEE, Vol. 54, pp. 1312–1328, 1966.

[41] R. G. Jones, "Precise dielectric measurements at 35 GHz using an open microwave resonator", IEE Proc., Vol. 123, pp. 285–290, 1976.

[42] R. N. Clarke and C. B. Rosenberg, "Fabry-Perot and open resonators at microwave and millimeter wave frequencies, 2-300 GHz", J. Phys. E.: Sci. Instrum., Vol. 15, no. 9, pp. 9–24, 1982.

[43] H. E. Bussey, J. E. Gray, E. C. Bamberger, E. Rushton, G. Russell, B. W. Petley, and D. Morris, "International comparison of dielectric measurements", IRE Trans. Instrum. Meas., Vol. IM-13, pp. 305–311, December 1964.

Manuscript was received on 19 June 1997, in revised form 31 March 1998.